Electronic Supplementary Material (ESI) for Dalton Transactions.

Structural Diversity in Pyridine and Polypyridine Adducts of Ring Slipped Manganocene: Correlating Ligand Steric Bulk with Quantified Deviation from Ideal Hapticity

Anthony F. Cannella,[a] Suman Kr Dey,[a] Samantha N. MacMillan,[a] David C. Lacy*[a]

a Department of Chemistry, University at Buffalo, Buffalo, New York 14260-3000, United States
b Department of Chemistry and Chemical Biology, Baker Laboratory, Cornell University, Ithaca, New York 14853, United States
E-mail: DCLacy@Buffalo.edu

Contents

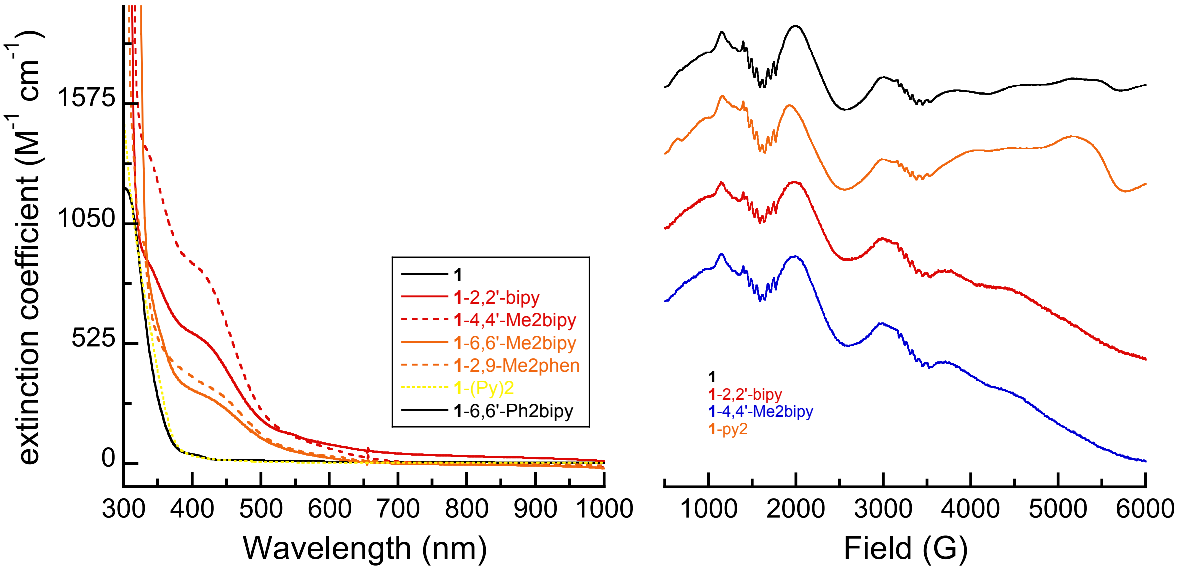

Figure S1. Left: Representative UV-vis spectra of **1**-L adducts in THF (concentration shown 0.75 mM). Reported extinction coefficients were determined using a Beer's law plot. Right: X-band EPR spectra of **1** (6 K, 35 dB), **1**-py$_2$ (6 K, 35 dB), **1**-2,2′-bipy (15 K, 35 dB), and **1**-4,4′-Me$_2$bipy (15 K, 35 dB) complexes in toluene.

X-ray Crystallography

Low-temperature (223 K) X-ray diffraction data for **1**-4,4′-Me$_2$bipy, **1**-6,6′-Me$_2$bipy, **1**-4,7-Ph$_2$phen, **1**-2,9-Me$_2$phen and **1**-py$_2$ were collected on a Bruker X8 Kappa diffractometer coupled to an ApexII CCD detector with graphite-monochromated Mo Kα radiation (α = 0.71073 Å) at Cornell University. The structures were solved through intrinsic phasing using SHELXT[1] and refined against F^2 on all data by full-matrix least squares with SHELXL[2] following established refinement strategies.[3] All non-hydrogen atoms were refined anisotropically. Hydrogen atoms bound to carbon were included in the models at geometrically calculated positions and refined using a riding model. The isotropic displacement parameters of all hydrogen atoms were fixed to 1.2 times the U value of the atoms they are linked to (1.5 times for methyl groups). For both **1**-2,9-Me$_2$phen and **1**-6,6′-Me$_2$bipy, two disordered solvent molecules of THF were included in the unit cell but could not be satisfactorily modeled. Therefore, that solvent was treated as a diffuse contribution to the overall scattering without using specific atom positions by the SQUEEZE function in PLATON[4].

X-ray crystallographic data for complexes **1**-bipy, **1**-phen and **1**-terpy were collected at The University at Buffalo using a Bruker SMART APEX2 CCD diffractometer installed at a rotating anode source (Mo$K\alpha$ radiation, α=0.71073 Å). The crystals were kept at 90(2) K during data collection using an Oxford Cryosystems nitrogen gas-flow apparatus. The structure was solved using Olex2[5] with the ShelXS[1] structure solution program using Direct Methods and refined with the ShelXL[2] refinement package using Least Square minimization. All non-hydrogen atoms were refined anisotropically. For all the three complexes the hydrogen atoms were calculated and fixed using SHELXL-97 after hybridization of all non-hydrogen atoms. The crystal lattice of **1**-bipy and **1**-terpy contain trapped and disordered THF molecules. These electron densities moved during refinement and could not be modeled properly and hence the lattice solvent molecules prohibited the convergence of the structures. Therefore, the Squeeze technique in Olex2 was used to subtract their contribution from the diffraction pattern.

Crystallographic details and selected bond distances and angles of all the complexes were summarized in Tables S2-S3.

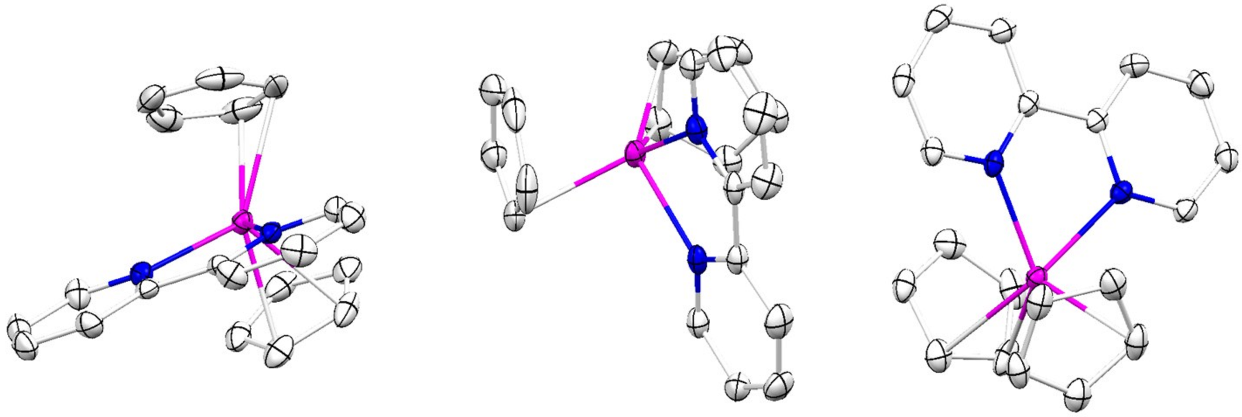

Figure S2. Thermal ellipsoid (50% probability) plot for complex **1**-bipy. Hydrogen atoms are omitted for clarity

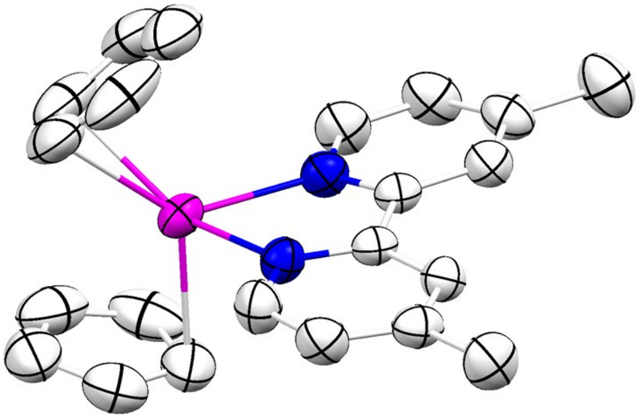

Figure S3. Thermal ellipsoid (50% probability) plot for complex **1**-4,4′-Me_2bipy. Hydrogen atoms are omitted for clarity

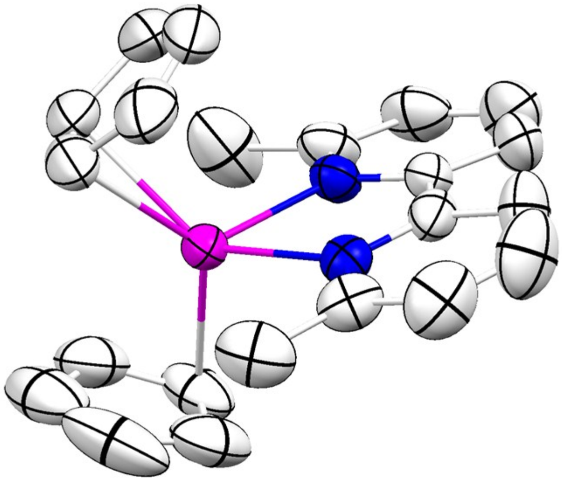

Figure S4. Thermal ellipsoid (50% probability) plot for complex **1**-6,6′-Me_2bipy. Hydrogen atoms and THF molecule are omitted for clarity

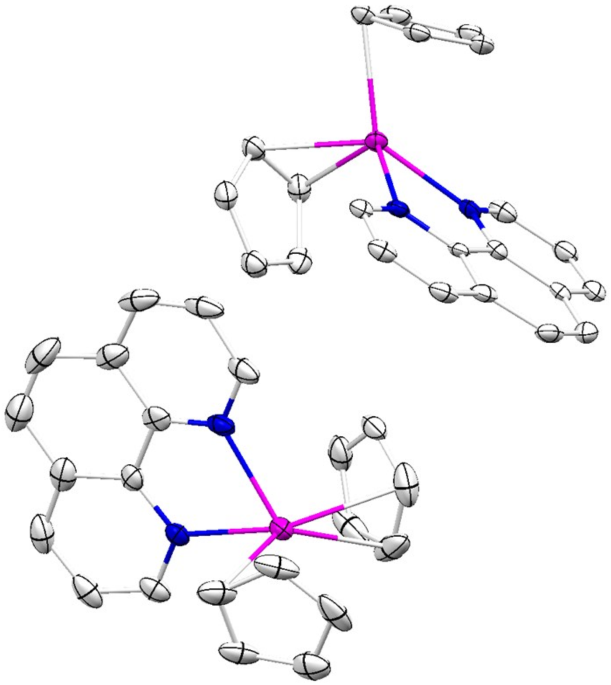

Figure S5. Thermal ellipsoid (50% probability) plot for complex **1**-phen. Hydrogen atoms are omitted for clarity.

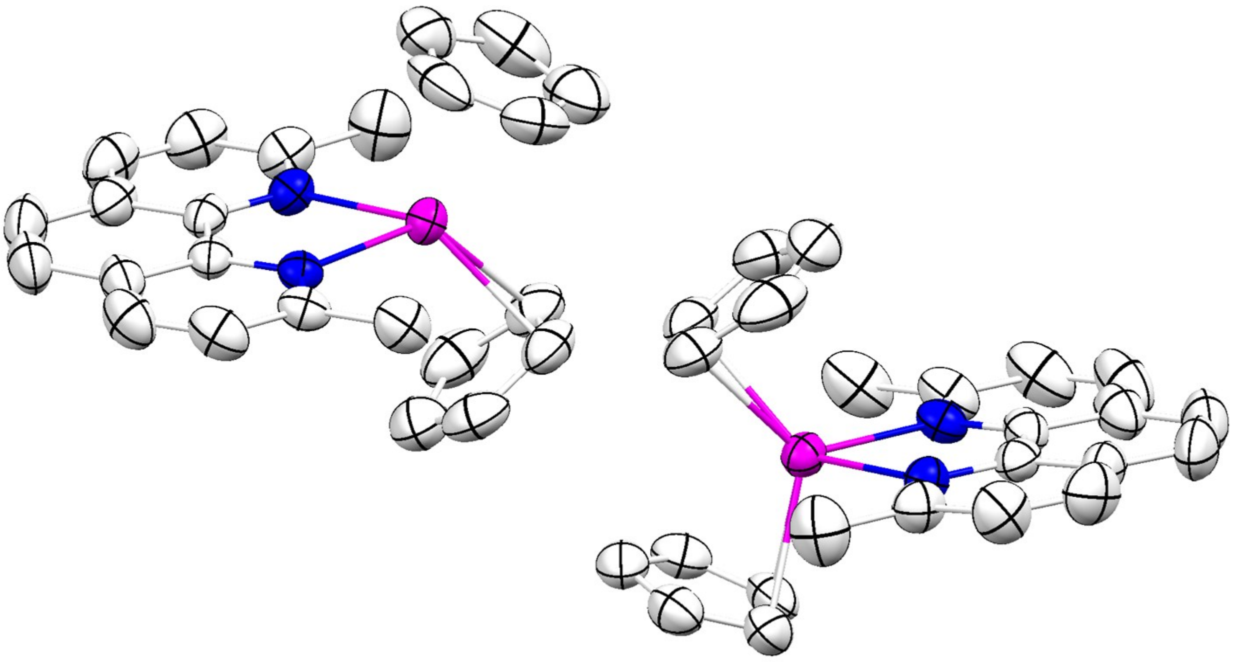

Figure S6. Thermal ellipsoid (50% probability) plot for complex **1**-2,9-Me$_2$phen. Hydrogen atoms are omitted for clarity.

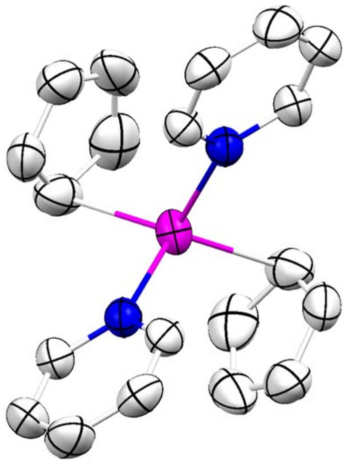

Figure S7. Thermal ellipsoid (50% probability) plot for complex **1**-py$_2$. Hydrogen atoms are omitted for clarity.

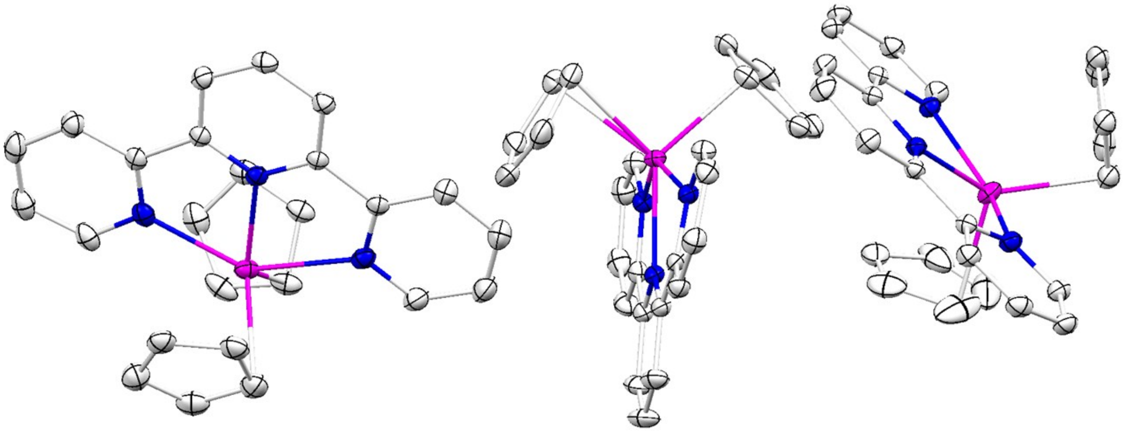

Figure S8. Thermal ellipsoid (50% probability) plot for complex **1**-terpy. Hydrogen atoms and THF solvent molecules are omitted for clarity.

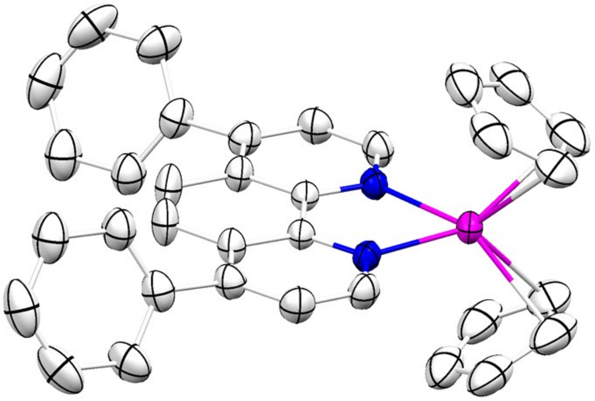

Figure S9. Thermal ellipsoid (50% probability) plot for complex **1**-4,7-Ph$_2$phen. Hydrogen atoms are omitted for clarity.

Table S1. Crystallographic parameters for **1**-bipy, **1**-4,4′-Me$_2$bipy, **1**-6,6′- Me$_2$bipy, and **1**-phen.

	3(**1**-bipy)	**1**-4,4′-Me$_2$bipy	(**1**-6,6′- Me$_2$bipy)•THF	**1**-phen
Moiety formula	3($C_{20}H_{18}MnN_2$)	$C_{22}H_{22}MnN_2$	$C_{48}H_{52}Mn_2N_4O_1$	$C_{22}H_{18}N_2Mn$
M_w	1023.91	369.35	810.81	365.34
crystal system	Monoclinic	Monoclinic	Orthorhombic	Orthorhombic
space group	$C2/c$	$P2_1/c$	$P2_12_12$	$Pca2_1$
a (Å)	18.5006(8)	11.7577(14)	14.7987(8)	11.0154(6)
b (Å)	20.7775(10)	11.0932(14)	16.8841(9)	26.5037(15)
c (Å)	30.9290(13)	15.441(2)	8.5878(6)	11.5756(7)
α (°)	90	90	90	90
β (°)	102.7317(14)	109.970(5)	90	90
γ (°)	90	90	90	90
V (Å^3)	11596.7(9)	1892.9(4)	2145.8(2)	3379.5(3)
Z	8	4	2	8
D_c (mg m^{-3})	1.173	1.296	1.255	1.436
μ (mm^{-1})	0.683	0.703	0.628	0.787
F (000)	5208	772	852	1512
R (int)	0.0552	0.0252	0.0204	0.0772
total reflections	98425	17051	13495	45577
unique reflections	16841	3716	5537	6871
$R1$, w$R2$ ($I \geq 2\sigma(I)$)	$R1$ = 0.0377, w$R2$ = 0.0848	$R1$ = 0.0344, w$R2$ = 0.0901	$R1$ = 0.0349, w$R2$ = 0.0894	$R1$ = 0.0450, w$R2$ = 0.0984
$R1$, w$R2$ (all data)	$R1$ = 0.0581, w$R2$ = 0.0922	$R1$ = 0.0426, w$R2$ = 0.0968	$R1$ = 0.0429, w$R2$ = 0.0935	$R1$ = 0.060, w$R2$ = 0.1045
temp (K)	90(2)	223(2)	223(2)	90(2)
goodness-of-fit	1.024	1.053	1.112	1.074
max. and min. trans.	0.942 and 0.877	0.7461 and 0.6747	0.7461 and 0.6619	0.896 and 0.854

Table S1 cont. Crystallographic parameters for **1**-4,7-Ph$_2$phen, **1**-2,9-Me$_2$phen, **1**-py$_2$, and **1**-terpy.

	1-4,7-Ph$_2$phen	**1** -2,9-Me$_2$phen	**1**-(py)$_2$	3(**1**-terpy)•3THF
Moiety formula	$C_{34}H_{26}MnN_2$	$C_{24}H_{22}MnN_2$	$C_{20}H_{20}MnN_2$	3[$C_{29}H_{29}MnN_3O$]
M_w	517.51	393.37	343.32	1471.48
crystal system	Tetragonal	Monoclinic	Orthorhombic	Triclinic
space group	$P\text{-}42_1c$	$P2_1/c$	$Aba2$	$P\text{-}1$
a (Å)	12.1372(7)	18.0321(7	7.8832(7)	14.905(2)
b (Å)	12.1372(7)	23.6980(9)	17.6630(19)	16.420(3)
c (Å)	21.6505(14)	13.6298(5)	12.5197(12)	16.608(3)
α (°)	90	90	90	93.364(4)
β (°)	90	100.457(2)°	90	91.606(4)
γ (°)	90	90	90	115.268(3)
V (Å^3)	3189.4(4)	5727.6(4)	1743.3(3)	3656.7(10)
Z	4	8	4	2
D_c (mg m^{-3})	1.078	0.912	1.308	1.336
μ (mm^{-1})	0.435	0.468	0.758	0.568
F (000)	1076	1640	716	1542
R (int)	0.0316	0.0394	0.0319	0.0436
total reflections	83057	51305	5214	50450
unique reflections	4117	10129	2092	23321
$R1$, w$R2$ ($I \geq 2\sigma(I)$	$R1$ = 0.0370, w$R2$ = 0.1084	$R1$ = 0.0352, w$R2$ = 0.0903	$R1$ = 0.0378, w$R2$ = 0.0869 [a]	$R1$ = 0.050, w$R2$ = 0.1148
$R1$, w$R2$ (all data)	$R1$ = 0.0409, w$R2$ = 0.1129	$R1$ = 0.0522, w$R2$ = 0.0969	$R1$ = 0.0511, w$R2$ = 0.0925	$R1$ = 0.0823, w$R2$ = 0.1318
temp (K)	223(2)	223(2)	223(2)	90(2)
goodness-of-fit	1.063	1.078	1.029	1.017
max. and min. trans.	0.7461 and 0.6979	0.7461 and 0.6884	0.7461 and 0.6610	0.945 and 0.873

Table S2. R^2 values for different crystallographically determined geometric quantities vs. adduct steric bulk.

Metric (x)[a]	Θ_T	$\%V_{bur}$
l	0.86	0.88
N	0.86	0.79
S	0.66	0.69
τ	0.62	0.65
$l * N$	0.93	0.92
$l * S$	0.68	0.72
$N * S$	0.69	0.72
$l * N$	0.93	0.92
$l * N * \cos\tau$	0.86	0.79
$l * N * \sin\tau$	0.70	0.72
l / N	0.57	0.63

a. x from equation 2 in manuscript.

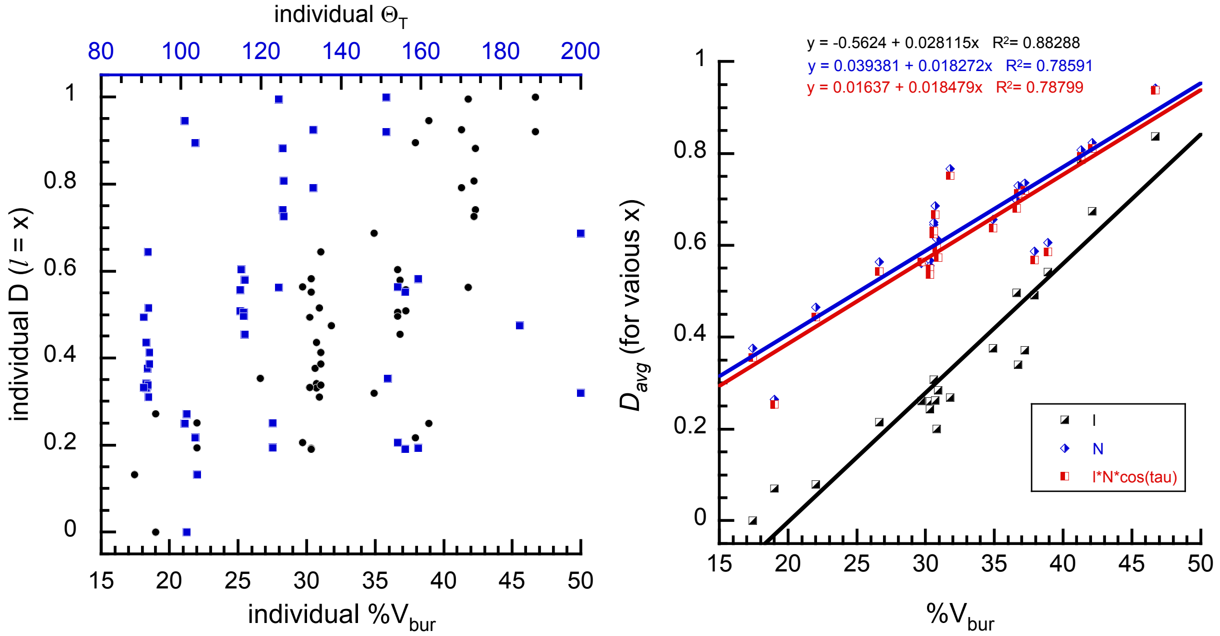

Figure S10. Left: Individual D values obtained from using x = $N*l$ in equation 2 of the manuscript plotted against steric bulk of the ligand (blue squares = cone angles; black dots = $\%V_{bur}$). Since the D values are not averaged across all the molecules in the unit cell, the steric parameters are not averaged as well and represent the values for the molecule for which the D value corresponds. Right: D_{avg} values calculated with some of the metrics in Table S2 vs. average $\%V_{bur}$.

1-bipy (Mn1)

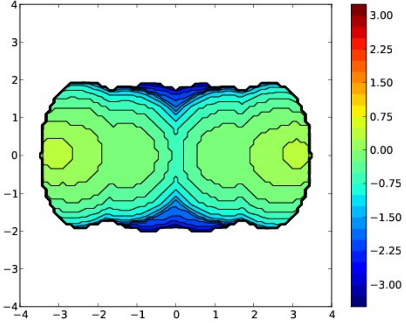

1-bipy (Mn2)

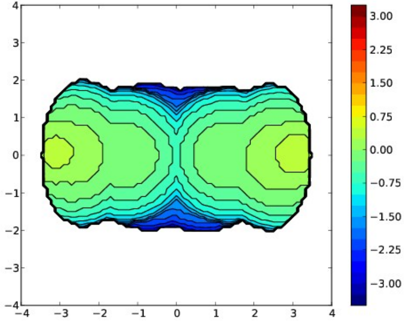

1-bipy (Mn3)

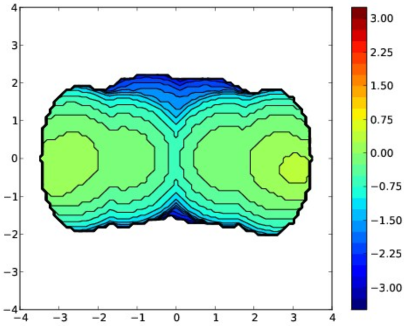

1-4,4'-Me_2bipy

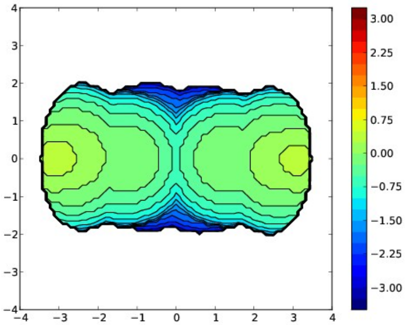

1-6,6'-Me_2bipy

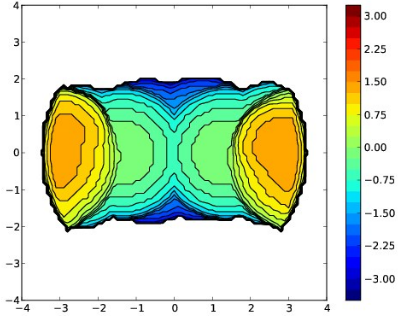

1-1,10-Phen (Mn1)

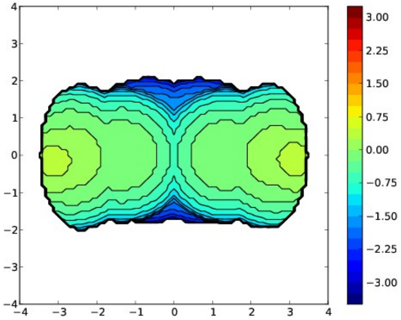

1-1,10-Phen (Mn2)

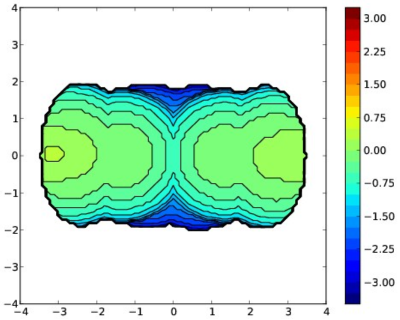

1-2,9-Me_2phen (Mn1)

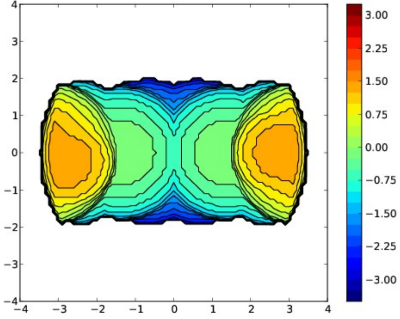

1-2,9-Me_2phen (Mn2)

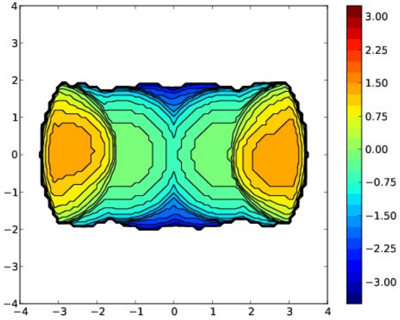

1-4,7-Ph_2phen

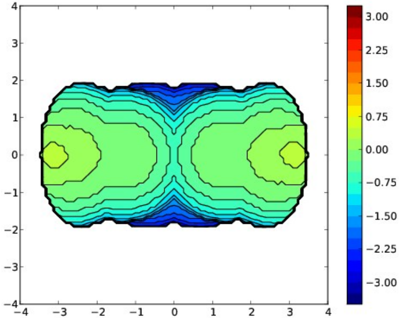

1-py_2 (both pyridine ligands)

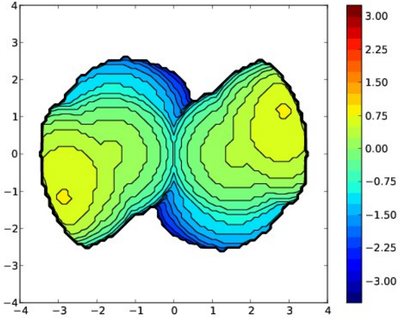

1-py_2 (only one pyridine ligand)

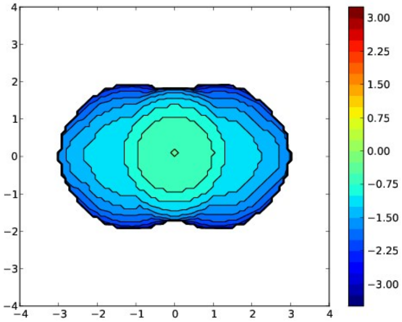

1-terpy (Mn1)

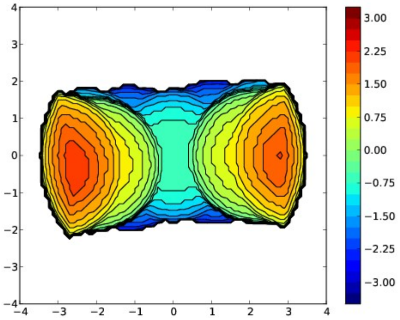

1-terpy (Mn2)

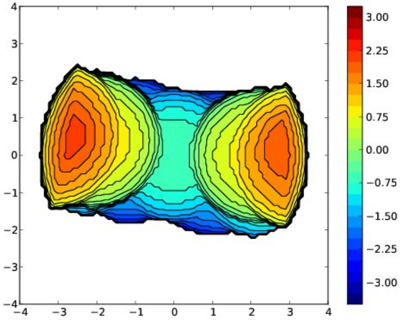

1-terpy (Mn3)

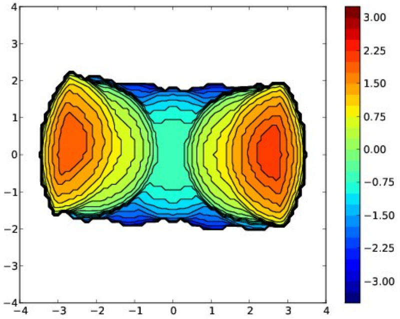

1-THF[6]

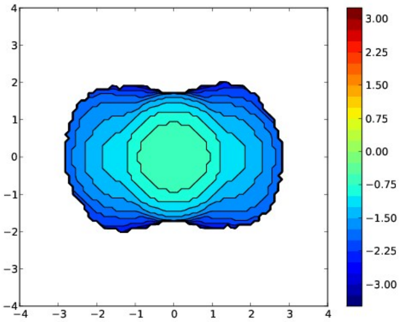

1-PMe$_3$[7]

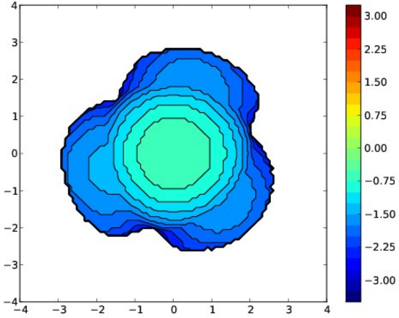

1-PPh$_2$Me[7]

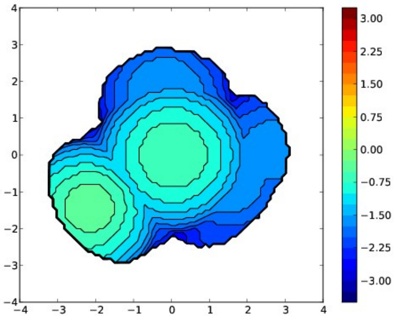

1-DMPE[7]

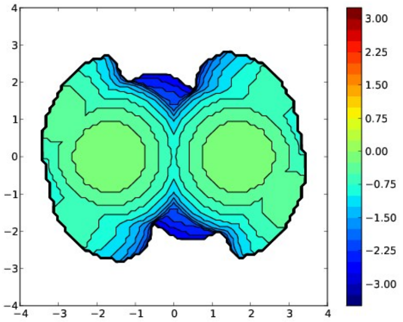

1-TMEDA[8]

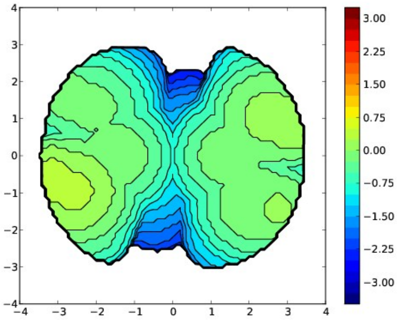

1-(TMG)$_2$[9]

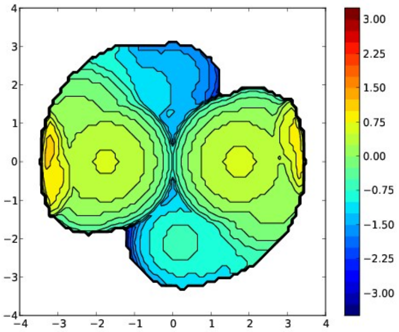

1-(TMG)$_2$ (only one TMG ligand)[9]

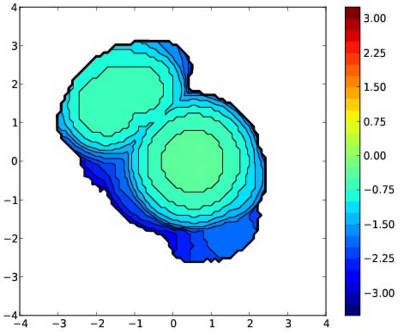

1- BzEDA[10]

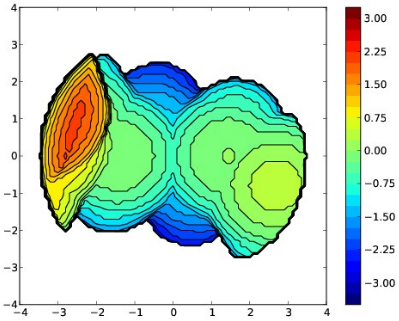

1-(NHC^{ArMe2Br}) [11]

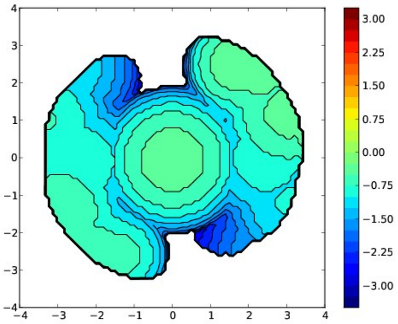

1-IMes[11]

1-(NHC^{Me4})$_2$**Error! Bookmark not defined.** (both ligands)

1-(NHC^{Me4})$_2$ (only one ligand)

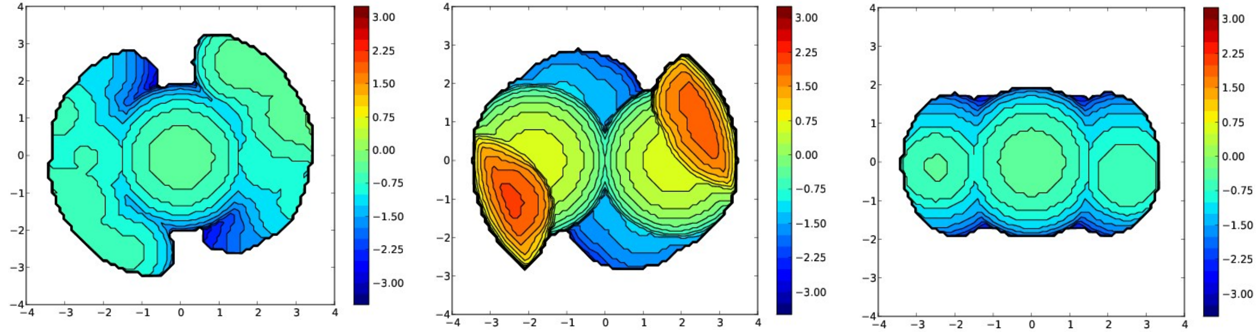

1-I*i*PrMe$_2$[12]

1- I*t*Bu[12]

1-IMes[12]

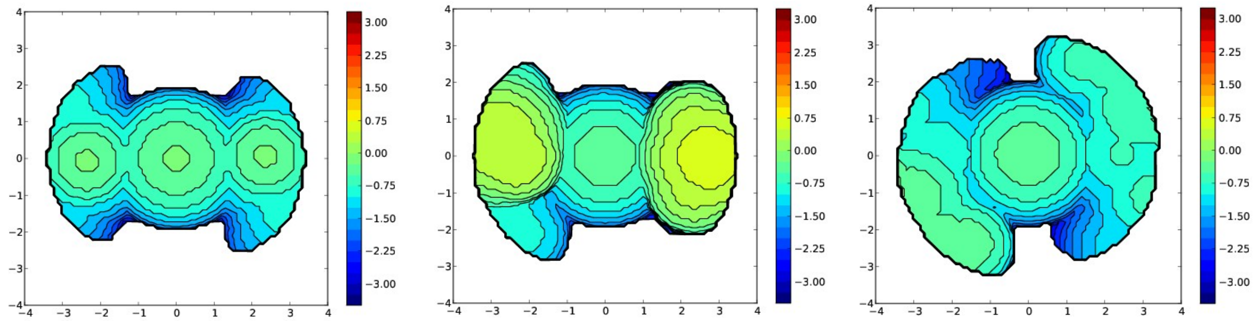

Figure S11. Steric maps determined for the **1**-L adducts based on XRD coordinates.

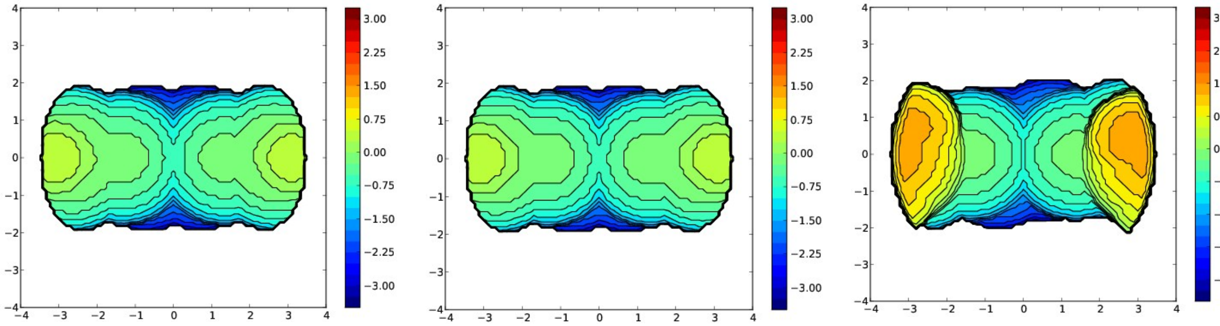

1-bipy (DFT) **1**-4,4'-Me_2bipy (DFT) **1**-6,6'-Me_2bipy (DFT)

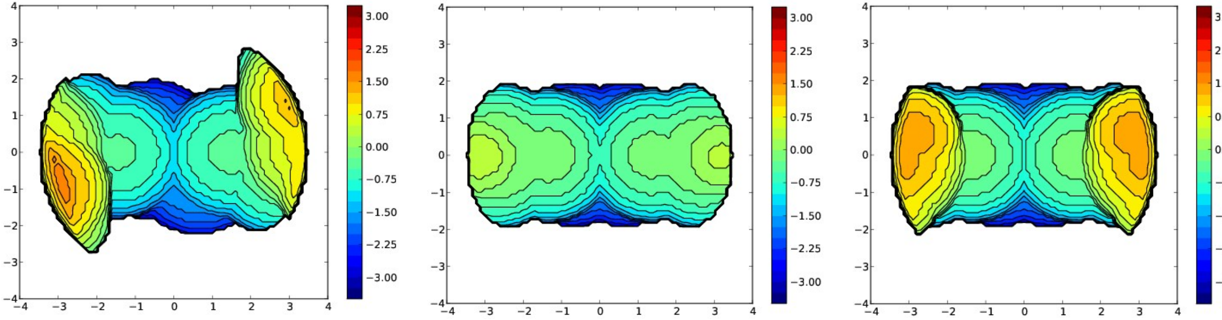

1-6,6'-Ph_2bipy (DFT) **1**-1,10-phen (DFT) **1**-2,9-Me_2phen (DFT)

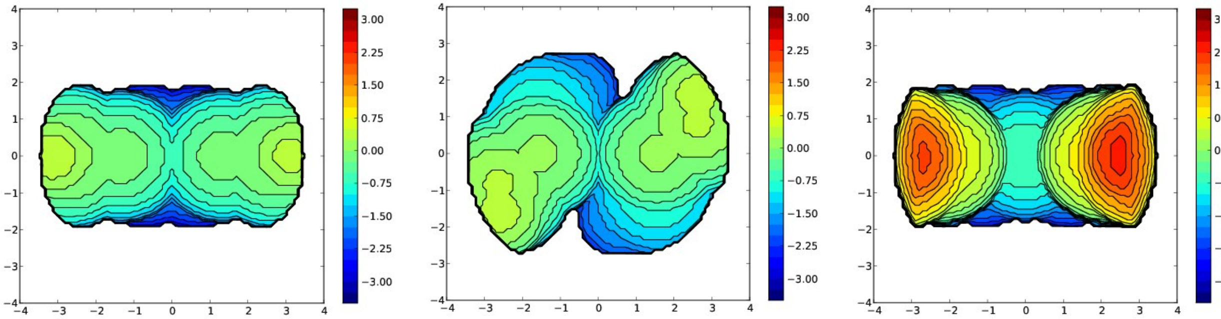

1-4,7-Ph_2phen (DFT) **1**-py_2 (DFT) **1**-terpy (DFT)

Figure S12. Steric maps determined for the **1**-L adducts based on DFT coordinates.

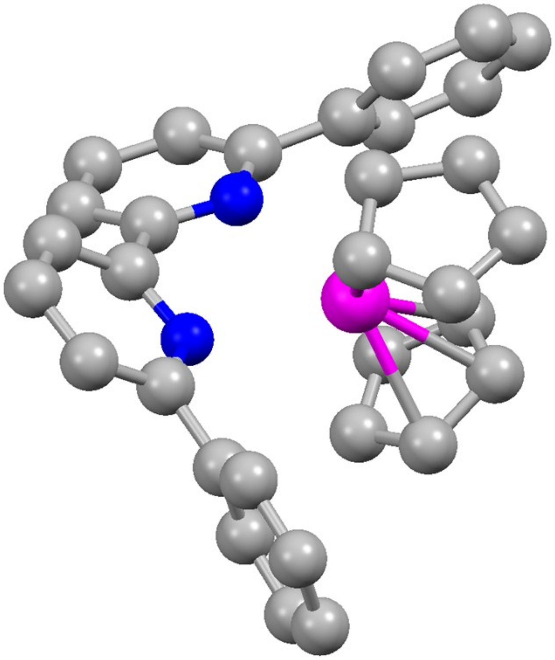

Figure S13. DFT optimized structure of **1**-6,6′-Ph_2bipy. Hydrogen atoms not displayed.

Density Functional Theory. All input files were generated using IQmol version 2.7.1 and calculations using Qchem version 4.4.[13] All reported geometry optimizations and frequency calculations were performed using a basis set of 6-31G* and the B3LYP functional and submitted to the Center for Computational Research (CCR) at the University at Buffalo. The initial input files for **1**-L adducts were generated using input from the solved XRD structures. In the case of multiple molecules per unit the Mn2 labeled molecule was chosen for the starting coordinates.

1. Sheldrick, G. M. *Acta Cryst.* **2015**, *A71*, 3-8.
2. Sheldrick, G.M. *Acta Cryst.* **2008**, *A64*, 112-122.
3. Müller, P. *Crystallography Reviews* **2009**, *15*, 57-83.
4. Spek, A. L. *Acta Cryst.* **2015**, *C71*, 9-18.
5. Dolomanov, O. V.; Bourhis, L. J.; Gildea, R. J.; Howard, J. A. K.; Puschmann, H. *J. Appl. Crystallogr.* **2009,** *42*, 339-341.
6. Bottomley, F.; Keizer, P. N.; White, P. S. Steric versus electronic effects on the “tilt” of the cyclopentadienyl rings in adducts of manganese dicyclopentadienide. Molecular and electronic struc-ture of dicyclopentadienide manganese tetrahydrofuran. J. Am. Chem. Soc. 1988, 110, 137-140.
7. Howard, C. G.; Girolami, G. S.; Wilkinson, G.; Thornton-Pett, M.; Hursthouse, M. B. Tertiary phosphine adducts of manganese(II) dicyclopentadienide. Magnet studies and structural char-acterization of “tilted” cyclopentadienyl rings. J. Am. Chem. Soc. 1984, 106, 2033-2040.
8. Heck, J.; Massa, W.; Weinig, P. TMEDA adducts of CpMnCl and manganocene. *Angew. Chem.*, *Int. Ed.* **1984**, *23*, 722-723.
9. Alvarez, C. S.; Boss, S. R.; Burley, J. C.; Humphry, S. M.; Lay-field, R. A.; Kowenicki, R. A.; McPartlin, M.; Rawson, J. M.; Wheatley, A. E. H.; Wood, P. T.; Wright, D. S. Syntheses, struc-tures and magnetic properties of Mn(II) dimers [CpMn(μ-X)]2 (Cp = C5H5; X = RNH, R1R2N, CCR) Dalton Trans. 2004, 3481-3487.
10. Alvarez, C. S.; Bashall, A.; Bond, A. D.; Clave, D.; Harron, E. A.; Layfield, R. A.; Mosquera, M. E. G.; McPartlin, M.; Rawson, J. M.; Wood, P. T.; Wright, D. S. Applications of manganocene in synthesis the synthesis of Mn(II) amide and imide cages. *Dalton Trans.* **2003**, 3002-3008.
11. Abernethy, C. D.; Cowley, A. H.; Jones, R. A.; Macdonald, C. L. B.; Shukla, P.; Thompson, L. K. Nucleophilic carbene complexes of manganocene Organometallics 2001, 20, 3629-3631.
12. Walter, M. D.; Baabe, D.; Freytag, M.; Jones, P. G. N-heterocyclic carbene (NHC) adducts of [(C5H5)2Mn] revisited: Nothing more, nothing less than high-spin (S = 5/2) molecules! Z. Anorg. Allg. Chem. 2016, 642, 1259-1263.
13. Shao, Y. H.; Gan, Z. T.; Epifanovsky, E.; Gilbert, A. T. B.; Wormit, M.; Kussmann, J.; Lange, A. W.; Behn, A.; Deng, J.; Feng, X. T.; Ghosh, D.; Goldey, M.; Horn, P. R.; Jacobson, L. D.; Kaliman, I.; Khaliullin, R. Z.; Kus, T.; Landau, A.; Liu, J.; Proynov, E. I.; Rhee, Y. M.; Richard, R. M.; Rohrdanz, M. A.; Steele, R. P.; Sundstrom, E. J.; Woodcock, H. L.; Zimmerman, P. M.; Zuev, D.; Albrecht, B.; Alguire, E.; Austin, B.; Beran, G. J. O.; Bernard, Y. A.; Berquist, E.; Brandhorst, K.; Bravaya, K. B.; Brown, S. T.; Casanova, D.; Chang, C. M.; Chen, Y. Q.; Chien, S. H.; Closser, K. D.; Crittenden, D. L.; Diedenhofen, M.; DiStasio, R. A.; Do, H.; Dutoi, A. D.; Edgar, R. G.; Fatehi, S.; Fusti-Molnar, L.; Ghysels, A.; Golubeva-Zadorozhnaya, A.; Gomes, J.; Hanson-Heine, M. W. D.; Harbach, P. H. P.; Hauser, A. W.; Hohenstein, E. G.; Holden, Z. C.; Jagau, T. C.; Ji, H. J.; Kaduk, B.; Khistyaev, K.; Kim, J.; Kim, J.; King, R. A.; Klunzinger, P.; Kosenkov, D.; Kowalczyk, T.; Krauter, C. M.; Lao, K. U.; Laurent, A. D.; Lawler, K. V.; Levchenko, S. V.; Lin, C. Y.; Liu, F.; Livshits, E.; Lochan, R. C.; Luenser, A.; Manohar, P.; Manzer, S. F.; Mao, S. P.; Mardirossian, N.; Marenich, A. V.; Maurer, S. A.; Mayhall, N. J.; Neuscamman, E.; Oana, C. M.; Olivares-Amaya, R.; O'Neill, D. P.; Parkhill, J. A.; Perrine, T. M.; Peverati, R.; Prociuk, A.; Rehn, D. R.; Rosta, E.; Russ, N. J.; Sharada, S. M.; Sharma, S.; Small, D. W.; Sodt, A.; Stein, T.; Stuck, D.; Su, Y. C.; Thom, A. J. W.; Tsuchimochi, T.; Vanovschi, V.; Vogt, L.; Vydrov, O.; Wang, T.; Watson, M. A.; Wenzel, J.; White, A.; Williams, C. F.; Yang, J.; Yeganeh, S.; Yost, S. R.; You, Z. Q.; Zhang, I. Y.; Zhang, X.; Zhao, Y.; Brooks, B. R.; Chan, G. K. L.; Chipman, D. M.; Cramer, C. J.; Goddard, W. A.; Gordon, M. S.; Hehre, W. J.; Klamt, A.; Schaefer, H. F.; Schmidt, M. W.; Sherrill, C. D.; Truhlar, D. G.; Warshel, A.; Xu, X.; Aspuru-Guzik, A.; Baer, R.; Bell, A. T.; Besley, N. A.; Chai, J. D.; Dreuw, A.; Dunietz, B. D.; Furlani, T. R.; Gwaltney, S. R.; Hsu, C. P.; Jung, Y. S.; Kong, J.; Lambrecht, D. S.; Liang, W. Z.; Ochsenfeld, C.; Rassolov, V. A.; Slipchenko, L. V.; Subotnik, J. E.; Van Voorhis, T.; Herbert, J. M.; Krylov, A. I.; Gill, P. M. W.; Head-Gordon, M., Advances in molecular quantum chemistry contained in the Q-Chem 4 program package. Mol. Phys. 2015, 113 (2), 184-215.